COOLING OF INTERSTELLAR FORMALDEHYDE BY COLLISION WITH HELIUM: AN ACCURATE QUANTUM MECHANICAL CALCULATION

Contents

COOLING OF INTERSTELLAR FORMALDEHYDE BY COLLISION WITH HELIUM: AN ACCURATE QUANTUM MECHANICAL CALCULATION

Barbara Jane Garrison

Inorganic Materials Research Division, Lawrence Berkeley Laboratory
and Department of Chemistry; University of California,
Berkeley, California 94720

ABSTRACT

In order to test a collisional pumping model as a mechanism for cooling the 6 cm and 2 cm doublets of interstellar formaldehyde, a quantum mechanical scattering calculation is performed. To obtain the intermolecular interaction between $H_2CO(^1A_1)$ and $He(^1S)$ two calculations are performed, a Hartree-Fock (HF) potential surface and a configuration interaction (CI) surface. A basis set of better than "triple zeta plus polarization" quality is used to compute the HF portion of the potential energy surface. This portion is highly anisotropic and has a slight attraction arising from induction effects at intermolecular separations around 9 a.u. The HF surface is modified through a series of CI calculations. Correlation is found to have little effect in the strongly anisotropic repulsive region of the interaction potential but dominates the well and long-range regions. The maximum well depth is attained for in-plane approaches of He and lies in the range 35-40°K for arbitrary θ at center of mass separation of 7.5 a.u. The entire surface is fit to a spherical harmonic expansion to facilitate scattering applications.

An Arthurs and Dalgarno type coupled channel (CC) formalism is presented for scattering of an asymmetric top by an atom. These CC equations are integrated at 12 scattering energies between 20 and 95°K.

For the cross section calculations a basis set of 16 ortho H_2CO states are included, resulting in 62 channels. Resonances are observed at ~20.2, 32.7 and 47.7°K. The cross sections are Boltzmann averaged to obtain rate constants which are used to solve the equations of statistical equilibrium. The 6 cm and 2 cm doublets of interstellar H_2CO are found to be cooled by collisions with He. The $j = 3$ ortho doublet plays a fundamental role in the cooling of H_2CO.

I. INTRODUCTION

During the past few years, considerable interest has developed around observations of anomalous absorption in interstellar formaldehyde. Because this absorption is seen toward dark clouds, it is anomalous, implying an excitation temperature for two rotational states lower than either the background radiation temperature (~2.7°K) or the expected kinetic temperature (10-20°K). These observations are quite common in the interstellar medium and are seen in (1) the $1_{10} - 1_{11}$ (6 cm) transition of H_2CO,[7,24,27] (2) the $2_{11} - 2_{12}$ (2 cm) transition of H_2CO,[10,12,13] and (3) the $1_{10} - 1_{11}$ transition of the isotope $H_2{}^{13}CO$.[13]

To obtain such low excitation temperatures requires a nonthermal cooling mechanism. A number of pumping models have been proposed that involve transitions to higher rotational states of H_2CO followed by radiative decay. The pump or force causing the excitations has been variously suggested as being due to collisions[35] or to radiation at millimeter,[32,34a] infrared,[22] and ultraviolet[25] wavelengths. Evans, et al.[13] have recently given a convincing discussion which indicates that the collisional pump is the only model that accounts for all the observations and satisfies necessary criteria.

The collisional pumping model of Townes and Cheung[35] is based on classical arguments. The rotational energy level structure and dipole allowed transitions of ortho H_2CO are shown in Fig. 4.1. Note that the lower levels of each doublet are connected by dipole allowed transitions; likewise, the upper levels. Thus, if a molecule is excited to state 3 (2_{12}) it will radiate to state 1 (1_{11}). The classical model proposes that both of the lower two states (j = 1 doublet) are preferentially

excited by collisions to state 3 where the molecule will radiatively decay to state 1, therefore, cooling the 6 cm (j = 1) doublet. (The intra-doublet relaxation is slow due to the small energy separation between the levels.)

Since the collisional pump appears to be the key to understanding interstellar cooling of H_2CO, several workers[2,10,11,13,34,35] have attempted to theoretically verify this model by determining the appropriate rotational cross sections. These calculations have been carried out subject to a number of limitations, including approximate interaction potentials (hard or soft sphere), approximate dynamics (classical or semi-classical calculations), and other less appropriate approximations (born or sudden).

In the present study the test of the collisional pump is based upon entirely quantum mechanical calculations. An accurate ab-initio interaction potential (Hartree-Fock and configuration interaction) between H_2CO and He is given in Chapters II and III. For these calculations, the most probable scatterer H_2 is replaced by He to reduce the scope of the computation. It is anticipated that the main conclusions of this study will not be seriously altered by this choice of scattering particle. In Chapter IV the Arthurs and Dalgarno[1] type coupled channel (CC) formalism is presented for scattering of an asymmetric top by an atom. Using the ab-initio potential, the CC equations are integrated to yield rotational cross sections. Collisional rates are then determined (in Chapter V) from these cross sections and used to test the validity of the collisional pump as a mechanism for the cooling of interstellar H_2CO.

II. HARTREE-FOCK INTERACTION POTENTIAL

A. Introduction

This chapter deals with the determination of the Hartree-Fock (HF) portion of the interaction potential (to be used in the scattering study) between H_2CO ($^1A_1$) and He (^1S). Because collision energies in interstellar space are small (≤100°K) and the vibrational energy level spacings of H_2CO are sufficiently large (>1600°K for the lowest fundamental), H_2CO should be well approximated by a rigid rotor. Consistent with the rigid rotor model, H_2CO is constrained to a single geometry in the calculations to be described. This results in a smaller number of degrees of freedom that must be treated and thereby significantly reduces the number of points needed to map the region of the interaction potential required for scattering studies.

At long range, the dispersion energy dominates the interaction of He with H_2CO. Lesk[20] has recently proven that the dispersion energy is unobtainable in the HF approximation so that a reliable determination of the correlation energy contribution is required for scattering studies of the present system. Nevertheless, it is clear that the HF method can accurately characterize the repulsive anisotropy of atom-diatomic molecule interactions between closed shell systems and yield quantitatively the induction energy at long range for such systems.[21] The present chapter forms the first of a two-part effort in which the second part--the determination of the dispersion interaction--will be presented in the following chapter.

B. Description of Calculations

Hartree-Fock calculations were carried out following the Roothaan approach with H_2CO constrained to the equilibrium geometry of R_{CO} = 1.208Å, R_{CH} = 1.116Å, and ∠HCH = 116°31' determined by Takagi and Oka.[33] To facilitate collision studies, interaction energies are presented in a coordinate system with origin at the center-of-mass (c.m.) of H_2CO that is shown in Fig. 2.1.

The choice of basis set was governed by two criteria. One is that the superposition error[36] be small. The other is that the quantities which determine the leading terms of the induction contribution to the interaction energy at long range (permanent moments of H_2CO, dipole polarizability of He) be reliably characterized.[4]

To test these criteria, preliminary calculations were performed with He constrained to θ = 0° (O-atom end) and θ = 180° (C-atom end) approaches to H_2CO, i.e., C_{2v} geometries. Table II.1 lists interaction energies obtained (1) in the HF model employing the basis sets used in our recent study[15] of ground and excited state properties of H_2CO, and (2) using the multipole theory expression given in the Appendix. The excellent agreement (within 0.1°K) for R ≥ 11 a.u. between energies computed using both basis sets and perturbation theory indicates that the induction contribution is quite well described and furthermore that the onset of the non-overlap region occurs for R ≈ 11 a.u.

Table II.2 lists basis sets A and B for the (H_2CO, He) system. The H_2CO basis sets have been described previously.[15] The He basis sets are due to van Duijneveldt[8] augmented by p functions chosen to give an accurate dipole polarizability.[37] The latter functions are required to

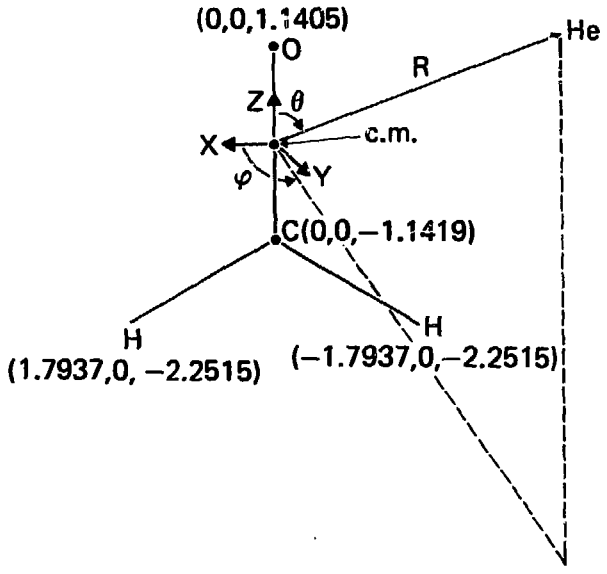

XBL 758-6877

Fig. 2.1. Coordinate system and geometry for the H_2CO-He system. The triads in parenthesis are the x, y and z coordinates of the atoms.

Table II.1. Comparison of Hartree-Fock and multipole expansion interaction energies (°K).*

R(a.u.)	Basis Set A**	Basis Set B†	Multipole Expansion
θ = 0°			
5.0	2508.83	2606.14	
6.0	228.96	276.60	
7.0	-11.05	20.58	
7.5	-22.29	1.83	-6.34
8.0	-18.65	-3.05	-4.30
8.5	-11.79	-3.61	-2.99
9.0	-6.33	-2.98	-2.12
9.5	-3.15	-2.15	-1.53
10.0	-1.[illegible]	-1.47	-1.13
11.0	-9.63	-0.69	-0.63
12.0		-0.36	-0.38
13.0		-0.22	-0.23
θ = 180°			
5.0	6355.97	6467.19	
6.0	777.87	838.07	
7.0	55.07	85.42	
7.5	4.13	21.36	
8.0	-6.91	1.78	-4.22
8.5	-7.13	-3.03	-2.93
9.0	-5.22	-3.29	-2.08
9.5	-3.39	-2.48	-1.51
10.0	-2.08	-1.67	-1.11
11.0	-0.77	-0.73	-0.63
12.0		-0.37	-0.37
13.0		-0.22	-0.23

*1°K = 3.1668×10^{-6} a.u.

**Obtained with formaldehyde geometry of Ref. 16.

†Obtained with formaldehyde geometry of Ref. 33. The energy differences are attributable to basis set; differences due to geometry are negligible.

Table II.2. Contracted Gaussian basis sets for H_2CO and He.*

Basis A

Atom	Type	Function*
O	S	0.006436(7816.54) + 0.048924(1175.82) + 0.233819(273.188) + 0.784798(81.1696)
	S	0.803381(27.1836) + 0.316720(3.4136)
	S	1.0(9.5322)
	S	1.0(0.9398)
	S	1.0(0.2846)
	X,Y,Z	0.040023(35.1832) + 0.253849(7.9040) + 0.806842(2.3051)
	X,Y,Z	1.0(0.7171)
	X,Y,Z	1.0(0.2137)
	X^2,Y^2,Z^2,XY,XZ,YZ	1.0(0.8)
C	S	0.006228(4232.61) + 0.047676(634.882) + 0.231439(146.097) + 0.789108(42.4974)
	S	0.791751(14.1892) + 0.321870(1.9666)
	S	1.0(5.1477)
	S	1.0(0.4962)
	S	1.0(0.1533)
	X,Y,Z	0.039196(18.1557) + 0.244144(3.9864) + 0.816775(1.1429)
	X,Y,Z	1.0(0.3594)
	X,Y,Z	1.0(0.1146)
	X^2,Y^2,Z^2,XY,XZ,YZ	1.0(0.8)
H	S	0.025374(48.442) + 0.189684(7.2835) + 0.852933(1.6517)
	S	1.0(0.46238)
	S	1.0(0.14587)
	X,Y,Z	1.0(1.0)

*Linear combinations are written in the form $C_1(\alpha_1) + C_2(\alpha_2) + \ldots$ where C_1,C_2, . . . are coefficients and α_1,α_2, . . . are Gaussian exponents.

Table II.2. Continued.

Atom	Type	Function
		Basis A
He	S	0.002600(233.093) + 0.019628(35.023) + 0.091421(7.9557) + 0.272853(2.2028)
	S	1.0(0.66435)
	S	1.0(0.20825)
	X,Y,Z	1.0(1.0000)
	X,Y,Z	1.0(0.2000)
		Basis B
O	S	0.000210(31195.6) + 0.001628(4669.38) + 0.008450(1062.62) + 0.034191(301.426) + 0.110311(98.5153)
	S	1.0(35.4609)
	S	1.0(13.6179)
	S	1.0(5.38618)
	S	1.0(1.53873)
	S	1.0(0.60550)
	S	1.0(0.22054)
	X,Y,Z	0.002266(114.863) + 0.017192(26.8767) 0.075341(8.32077)
	X,Y,Z	1.0(2.97237)
	X,Y,Z	1.0(1.12848)
	X,Y,Z	1.0(0.42360)
	X,Y,Z	1.0(0.15074)
	X^2,Y^2,Z^2,XY,XZ,YZ	1.0(2.0)
	X^2,Y^2,Z^2,XY,XZ,YZ	1.0(0.5)

Table II.2. Continued.

Basis B		
Atom	Type	Function
C	S	0.000242(15469.4) + 0.001879(2316.47) + 0.009743(527.099) + 0.039167(149.438) + 0.123636(48.8562)
	S	1.0(17.6209)
	S	1.0(6.81082)
	S	1.0(2.7276)
	S	1.0(0.75674)
	S	1.0(0.30073)
	S	1.0(0.11409)
	X,Y,Z	0.002734(51.7233) + 0.018979(12.3397) + 0.080806(3.77224)
	X,Y,Z	1.0(1.32487)
	X,Y,Z	1.0(0.50546)
	X,Y,Z	1.0(0.19827)
	X,Y,Z	1.0(0.07731)
	X^2,Y^2,Z^2,XY,XZ,YZ	1.0(2.0)
	X^2,Y^2,Z^2,XY,XZ,YZ	1.0(0.5)
H	S	0.002006(82.636374) + 0.015345(12.409558) + 0.075577(2.823854)
	S	1.0(0.797670)
	S	1.0(0.258053)
	S	1.0(0.089891)
	X,Y,Z	1.0(1.0)
He	S	0.000059(4840.888547) + 0.000463(723.108918) + 0.002422(164.299706) + 0.009995(46.636262) + 0.034249(15.277787) + 0.096302(5.526897)
	S	1.0(2.132879)
	S	1.0(0.849674)
	S	1.0(0.343643)
	S	1.0(0.138709)
	X,Y,Z	1.0(1.0)
	X,Y,Z	1.0(0.2)

yield a proper description of the induction contribution to the interaction energy at long range. Figure 2.2 plots the interaction energy for C_{2v} approaches of He to the O-atom end ($\theta = 0°$) and C-atom end ($\theta = 180°$) for basis sets A and B and indicates the magnitude of the superposition error that accompanies the use of basis set A. Basis set B reduces the superposition error to approximately half the well depth. The close agreement between interaction energies obtained using basis set B and perturbation theory results given in Table II.1, and the reasonable agreement between the dipole moment determined employing basis set B and experiment, lend support to the notion that basis set B should provide a reliable description of the HF portion of the interaction potential.

C. Results and Discussion

Hartree-Fock interaction energies obtained using basis set B are presented in Table II.3 for $\phi = 0°$ (He incident in the plane of formaldehyde), in Table II.4 for $\phi = 30°$, in Table II.5 for $\phi = 60°$, and in Table II.6 for $\phi = 90°$ (He incident in the perpendicular bisector plane of H_2CO). Owing to H_2CO symmetry, only $0° \leq \phi \leq 90°$ need be considered. Because the interaction potantial is planned for scattering studies at energies $\leq$100°K, R = 5 a.u. was arbitrarily chosen as the minimum R for computations. At this separation, the interaction is exponential, with repulsion energies ranging up to several thousand degrees K; see Tables II.3-II.6. The maximum R treated was chosen as the onset of agreement between HF and perturbation theory induction energies which, as discussed in relation to Table II.1, occurs at ~11 a.u. Because of the large repulsion at $\theta \approx 140°$ due to the He-H interaction,

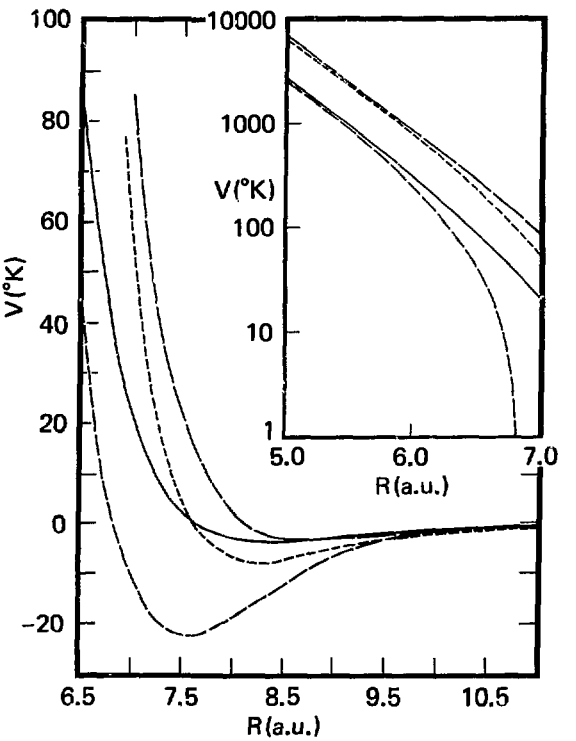

Fig. 2.2. Basis set dependence of the interaction energy for C_{2v} geometry: – – – Basis A for θ = 0°, ——— basis B for θ = 0°, ----- basis A for θ = 180°, — — — basis B for θ = 180°.

Table II.3. Interaction energies (°K) for ϕ = 0°.*

	R (a.u.)					
θ	5	6	7	8	9	10
0	2606.14	276.60	20.58	-3.05	-2.98	-1.47
30	2044.04	237.92	20.15	-3.26	-3.55	-1.66
60	837.23	101.05	6.60	-3.67	-2.67	-1.03
90	621.14	76.45	5.52	-1.52	-0.98	-0.37
120	7220.33	1178.99	169.48	21.63	2.02	-0.15
140	15852.93	2474.73	352.67	46.22	4.86	0.01
160	11942.20	1774.97	235.29	25.72	0.82	-0.86
180	6467.19	838.07	85.42	1.78	-3.29	-1.67

*See footnote * of Table II.1.

Table II.4. Interaction energies (°K) for ϕ = 30°.*

	R(a.u.)					
θ	5	6	7	8	9	10
30	1967.52	226.04	18.50	-3.12	-3.29	-1.56
60	840.15	102.82	7.62	-2.92	-2.32	-0.95
90	563.52	70.95	6.26	-0.74	-0.70	-0.33
120	4468.44	735.56	109.13	14.39	1.27	-0.22
140	10343.96	1642.55	236.61	30.93	2.91	-0.23
160	9735.36	1431.19	185.02	18.57	-0.18	-1.01

*See footnote * of Table II.1.

Table II.5. Interaction energies (°K) for ϕ = 60°.*

	R(a.u.)					
θ	5	6	7	8	9	10
30	1813.06	202.06	15.16	-2.83	-2.77	-1.35
60	830.64	103.06	8.69	-1.84	-1.77	-0.80
90	555.09	72.21	7.22	-0.21	-0.54	-0.31
120	1608.87	240.09	30.45	2.74	-0.32	-0.44
140	3942.97	590.33	75.57	6.93	-0.55	-0.73
160	6138.00	850.97	97.83	5.87	-2.03	-1.30

*See footnote * of Table II.1.

Table II.6. Interaction energies (°K) for ϕ = 90°.*

	R(a.u.)					
θ	5	6	7	8	9	10
30	1735.15	189.98	13.48	-2.70	-2.50	-1.25
60	819.62	101.86	8.84	-1.47	-1.53	-0.73
90	589.43	80.31	8.63	-0.06	-0.53	-0.31
120	888.84	115.70	11.74	0.09	-0.71	-0.46
140	2060.27	262.98	23.82	-0.87	-1.78	-0.93
160	4670.12	606.53	60.25	0.34	-2.86	-1.44

*See footnote * of Table II.1.

θ was sampled at the unevenly spaced values of 0, 30, 60, 90, 120, 140, 160 and 180°. A total of 156 energy points were computed using basis set B.

Figure 2.3 broadly summarizes the results contained in Tables II.3 through II.6 in the form of equipotential plots for He incident in (a) the H_2CO plane (ϕ = 0°) and (b) the perpendicular bisector plane (ϕ = 90°). For ϕ = 0°, a slight attraction at R ≈ 9 a.u. is evident as is the large repulsion at small R due to the H atom. At ϕ = 90°, however, the equipotential plot is very nearly symmetrical about θ = 90°. (Note that the opening of the zero contour is an artifact of having used the spherical harmonic expansion to generate the plots and reflects slight inaccuracies in the fit functions.) These and other features are more clearly shown in the planar projections presented in Figs. 2.4-2.7. The reduction of the strong repulsion due to the H atoms as He approaches for increasingly large out-of-(H_2CO) plane angles ϕ is detailed in Fig. 2.4 for R = 7 a.u., in Fig. 2.5 for R = 9 a.u., and in Fig. 2.6 for R = 10 a.u. Figure 2.7 presents another view of the R dependence of the interaction for He incident in the plane of H_2CO and shows the pronounced decline of the repulsion due to H at R ≈ 10 a.u. which portends the onset of the non-overlap region describable by multipole theory. From perturbation theory, the form of the long-range induction energy is $\cos^2\theta$. At R = 9 a.u. (Fig. 2.5), this functional behavior is perceptible in the bisector plane approach (ϕ = 90°). Note that by R = 10 a.u. (Fig. 2.6), the He-H interaction is much less repulsive and the long-range forces begin to dominate.

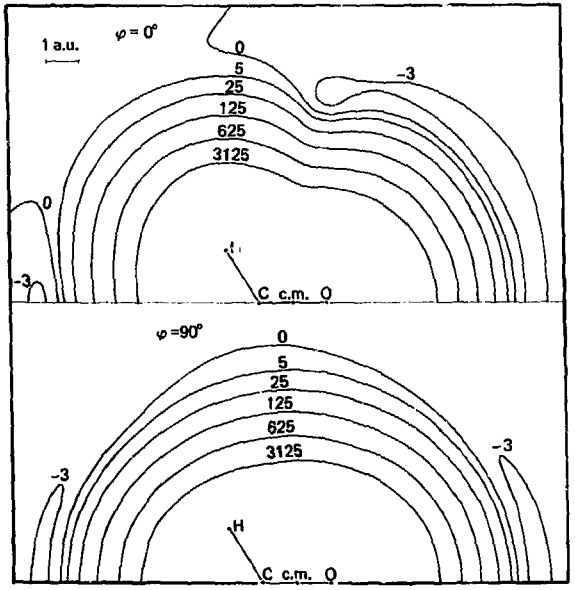

XBL 758-6875

Fig. 2.3. Contour plots of the interaction potential for He incident in the plane of H_2CO (ϕ = 0°) and He incident in the bisector plane (ϕ = 90°). Energies in °K. c.m. denotes center of mass.

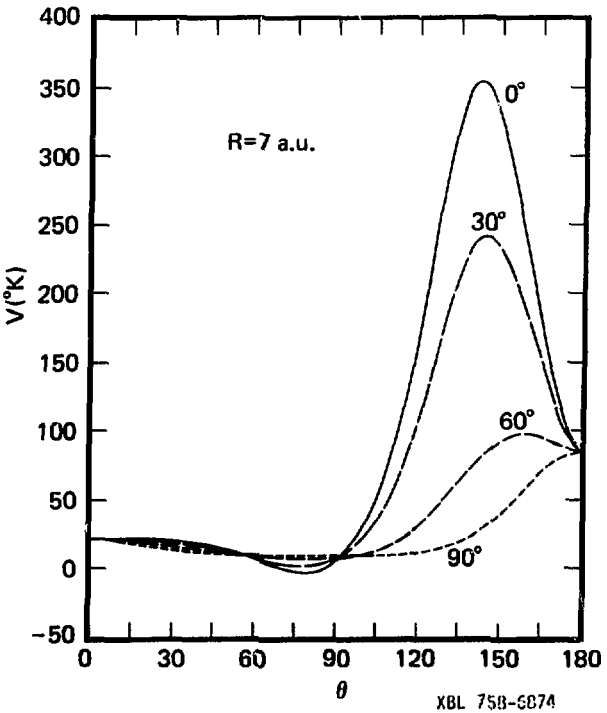

Fig. 2.4. Interaction energy vs θ for selected angles φ at R = 7 a.u.

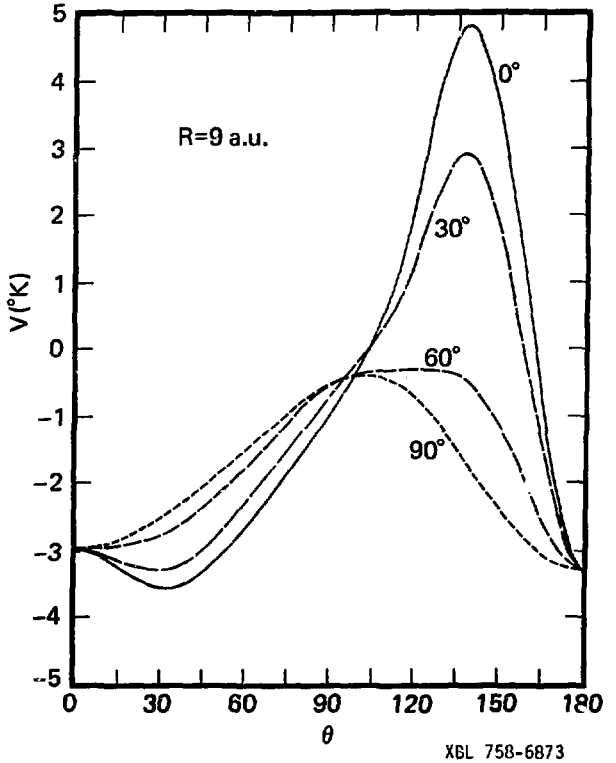

Fig. 2.5. Interaction energy vs θ for selected angles φ at R = 9 a.u.

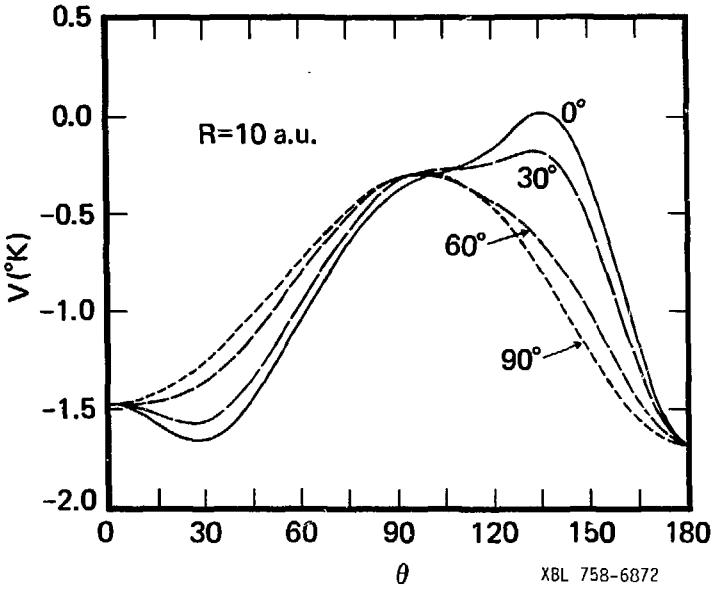

Fig. 2.6. Interaction energy vs θ for selected angles φ at R = 10 a.u.

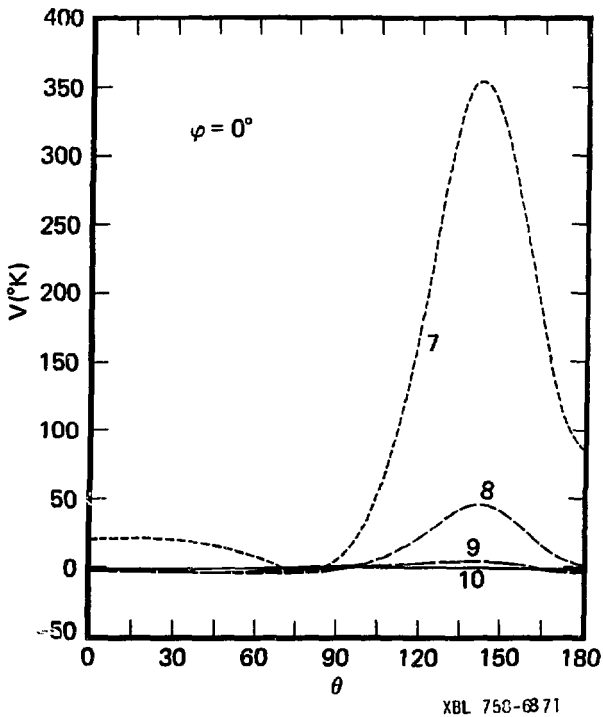

Fig. 2.7. Interaction energy vs θ for selected R at $\phi = 0°$.

The HF interaction energies obtained using basis set B have been fit to an expansion in spherical harmonics, viz.

$$V(R,\theta,\phi) = \sum_{\ell=0}^{\ell_{max}} \sum_{m=-\ell}^{\ell} (4\pi/2\ell+1)^{1/2} \quad v_{\ell m}(R)\ Y_{\ell m}(\theta,\phi) \quad . \qquad (1)$$

Ab initio energy points were supplemented by additional points determined by the method of splines to yield a dense grid to facilitate the determination of the radial coefficients. The HF energies were accurately reproduced using $\ell_{max} = 12$ by both least-squares and numerical integration procedures. Formaldehyde symmetry leads to $v_{\ell m}(R) = v_{\ell -m}(R)$, for m an even integer, and to 49 unique nonzero terms through $\ell = 12$. The $v_{\ell m}$ coefficients are given in Table II.7. These coefficients have been fit to the radial function

$$v_{\ell m}(R) = \begin{cases} A\, e^{-BR} - CR^{-6} - DR^{-7} & , R \leq 10.5 \text{ a.u.} \\ 0 & , R > 10.5 \text{ a.u.} \end{cases} \qquad (2)$$

A, B, C and D are listed in Table II.8.

D. Summary and Remarks

Using a basis set of better than triple zeta plus polarization quality, a Hartree-Fock interaction potential for the H_2CO-He system has been determined for fixed geometry of H_2CO suitable for rigid rotor scattering studies. The potential energy surface is highly anisotropic for He incident in the plane of H_2CO and has a small ($\lesssim 3°K$) minimum at $R \simeq 9$ a.u. The ab initio surface agrees closely with interaction energies determined from perturbation theory for $R \geq 11$ a.u., which is indicative of the onset of the non-overlap region.

Table II.7. Radial coefficients $v_{\ell m}(R)$ of spherical harmonic expression ($^{\circ}K$).

		R(a.u.)					
ℓ	m	5	6	7	8	9	10
0	0	2580.1	374.7	46.91	3.47	-0.93	-0.68
1	0	-3253.8	-531.2	-77.89	-11.50	-2.05	-0.41
2	0	3773.1	527.4	64.57	5.40	-0.83	-0.72
2	2	1144.5	188.8	27.81	3.48	0.29	0.01
3	0	-296.6	-20.8	2.79	2.39	1.00	0.24
3	2	-2139.1	-355.0	-54.02	-8.19	-1.35	-0.23
4	0	-1003.4	-208.0	-37.17	-6.22	-0.87	-0.09
4	2	2383.1	388.2	58.51	8.26	1.00	0.09
4	4	223.7	34.6	4.26	0.31	-0.02	0.00
5	0	1348.7	224.7	35.37	5.66	1.02	0.22
5	2	-1541.8	-241.5	-35.86	-5.39	-0.89	-0.17
5	4	-415.2	-63.7	-8.33	-0.98	-0.09	-0.01
6	0	-827.2	-134.2	-20.56	-3.25	-0.54	-0.09
6	2	764.2	115.6	17.03	2.50	0.35	0.05
6	4	457.9	66.6	8.65	1.05	0.11	0.01
6	6	32.0	3.4	-0.16	-0.15	-0.04	-0.01
7	0	290.0	48.4	7.50	1.12	0.20	0.05
7	2	-185.8	-30.0	-4.49	-0.67	-0.13	-0.03
7	4	-369.9	-49.5	-6.23	-0.73	-0.07	0.00
7	6	-63.1	-7.5	-0.06	0.18	0.04	0.01
8	0	51.8	4.9	0.50	0.14	0.05	0.02
8	2	-65.1	-8.2	-1.12	-0.21	-0.05	-0.01
8	4	253.6	32.6	4.05	0.48	0.05	0.00
8	6	73.1	8.5	0.32	-0.13	-0.03	-0.01
8	8	12.3	1.1	0.23	0.01	0.00	0.00
9	0	-101.9	-16.0	-2.44	-0.41	-0.07	-0.01
9	2	106.3	15.7	2.29	0.35	0.05	0.00
9	4	-145.5	-18.9	-2.37	-0.29	-0.03	0.00
9	6	-64.3	-6.9	-0.45	0.06	0.02	0.00

Table II.7. Continued.

		R(a.u.)					
ℓ	m	5	6	7	8	9	10
9	8	-23.9	-3.8	-0.51	-0.06	-0.01	0.00
10	0	39.9	6.0	0.90	0.17	0.03	0.00
10	2	-36.1	-5.3	-0.77	-0.12	-0.02	0.00
10	4	59.0	7.8	0.99	0.13	0.01	0.00
10	6	53.5	5.6	0.45	-0.02	-0.01	0.00
10	8	28.9	4.4	0.57	0.07	0.01	0.00
10	10	1.2	0.1	0.03	0.00	0.00	0.00
11	0	28.2	4.9	0.77	0.10	0.01	0.00
11	2	-25.5	-4.1	-0.62	-0.09	-0.01	0.00
11	4	-11.0	-1.5	-0.20	-0.03	0.00	0.00
11	6	-39.8	-4.2	-0.34	0.01	0.01	0.00
11	8	-29.4	-4.2	-0.54	-0.06	-0.01	0.00
11	10	-2.7	-0.5	-0.07	-0.01	0.00	0.00
12	0	-55.2	-9.3	-1.45	-0.22	-0.03	-0.01
12	2	49.2	7.7	1.15	0.17	0.03	0.00
12	4	-8.0	-1.0	-0.12	0.00	0.00	0.00
12	6	26.1	2.7	0.23	-0.01	0.00	0.00
12	8	28.0	3.9	0.49	0.06	0.01	0.00
12	10	3.7	0.6	0.09	0.01	0.00	0.00
12	12	0.0	0.0	0.00	0.00	0.00	0.00

Table II.8. Parameters for the HF interaction.*

ℓ	m	A**	B	C**	D**
0	0	3.034 (7)	1.845	-4.793 (6)	5.635 (7)
1	0	-2.483 (7)	1.751	1.226 (7)	-1.186 (8)
2	0	5.449 (7)	1.890	-6.558 (6)	7.320 (7)
2	2	8.094 (6)	1.735	-3.628 (6)	3.789 (7)
3	0	-1.056 (8)	2.586	-7.069 (5)	1.354 (6)
3	2	-1.546 (7)	1.736	8.259 (6)	-8.037 (7)
4	0	-3.534 (6)	1.535	9.527 (6)	-9.868 (7)
4	2	1.853 (7)	1.759	-6.595 (6)	6.644 (7)
4	4	1.891 (6)	1.774	-7.542 (5)	8.072 (6)
5	0	9.850 (6)	1.748	-3.935 (6)	3.771 (7)
5	2	-1.483 (7)	1.810	3.471 (6)	-3.309 (7)
5	4	-3.876 (6)	1.773	2.176 (6)	-2.133 (7)
6	0	-6.766 (6)	1.773	2.240 (6)	-2 139 (7)
6	2	9.097 (6)	1.867	-6.458 (5)	6.286 (6)
6	4	5.635 (6)	1.849	-1.443 (6)	1.405 (7)
6	6	1.054 (6)	2.084	-1.275 (5)	1.425 (6)
7	0	2.065 (6)	1.736	-9.935 (5)	9.736 (6)
7	2	-1.527 (6)	1.765	6.644 (5)	-6.362 (6)
7	4	-7.489 (6)	1.970	4.087 (5)	-4.048 (6)
7	6	-1.423 (6)	1.999	2.603 (5)	-2.759 (6)
8	0	6.528 (6)	2.340	-1.211 (5)	8.455 (5)
8	2	-2.540 (6)	2.123	-6.083 (3)	2.294 (5)
8	4	6.741 (6)	2.032	-1.058 (5)	1.096 (6)
8	6	2.284 (6)	2.072	-1.670 (5)	1.855 (6)
8	8	2.483 (6)	2.440	7.301 (4)	-6.220 (5)
9	0	-1.018 (6)	1.827	1.612 (5)	-1.453 (6)
9	2	1.458 (6)	1.900	-5.968 (5)	5.435 (5)
9	4	-3.530 (6)	2.011	9.729 (4)	-9.621 (5)
9	6	-3.142 (6)	2.154	7.576 (4)	-8.948 (5)
9	8	-1.829 (5)	1.749	9.982 (4)	-1.005 (6)

*Distance units are a.u. and energy units are °K.

**Values in parenthesis are powers of 10.

Table II.8. Continued.

ℓ	m	A**	B	C**	D**
10	0	5.618 (5)	1.909	-2.721 (4)	1.752 (5)
10	2	-5.311 (5)	1.916	1.599 (4)	-1.309 (5)
10	4	1.374 (6)	2.003	-4.401 (4)	4.150 (5)
10	6	3.146 (6)	2.191	-2.969 (4)	4.099 (5)
10	8	2.936 (5)	1.818	-8.167 (4)	8.218 (5)
10	10	1.088 (6)	2.730	9.658 (3)	-8.540 (4)
11	0	1.532 (5)	1.681	-9.677 (4)	1.023 (6)
11	2	-2.037 (5)	1.763	7.733 (4)	-7.618 (5)
11	4	-2.004 (5)	1.950	1.693 (4)	-1.453 (5)
11	6	-2.502 (6)	2.206	1.243 (4)	-2.111 (5)
11	8	-4.106 (5)	1.881	7.275 (4)	-7.134 (5)
11	10	-1.562 (4)	1.691	1.133 (4)	-1.127 (5)
12	0	-3.809 (5)	1.730	1.869 (5)	-1.840 (6)
12	2	4.697 (5)	1.811	-9.500 (4)	9.246 (5)
12	4	-1.694 (5)	1.982	2.674 (3)	-5.278 (4)
12	6	1.825 (6)	2.232	7.190 (2)	5.528 (4)
12	8	4.479 (5)	1.913	-5.518 (4)	5.421 (5)
12	10	2.446 (4)	1.734	-8.733 (3)	9.300 (4)
12	12	-2.358 (1)	1.273	3.639 (2)	-4.978 (3)

Since the Hartree-Fock model cannot describe dispersion contributions, which from perturbation theory should dominate the long-range interaction in the present system, correlation studies will be needed to complement results presented here.

APPENDIX

The induction contribution to the long range interaction between H_2CO and He may be written,[4]

$$V(R,\theta,\phi) = \sum_{\ell} \sum_{m} (4\pi/2\ell+1)^{1/2} \quad v_{\ell m}(R)\ Y_{\ell m}(\theta,\phi) \tag{A1}$$

The lowest order nonzero terms are

$$v_{00}(R) = -\mu^2\alpha/R^6 \tag{A2}$$

$$v_{20}(R) = v_{00}(R) \tag{A3}$$

$$v_{10}(R) = -18\ \mu\alpha\theta_{zz}/5R^7 \tag{A4}$$

$$v_{30}(R) = (2/3)\ v_{10}(R) \tag{A5}$$

$$v_{32}(R) = -\mu\alpha(8/15)^{1/2}\ (\theta_{xx} - \theta_{yy})/R^7 \tag{A6}$$

Here, α is the dipole polarizability of He, μ is the dipole moment of H_2CO, and θ_{ii} (ii $\equiv$ xx, yy and zz) are the diagonal components of the quadrupole moment tensor of H_2CO. Note that the dipole-induced dipole contribution (R^{-6}) is two orders of magnitude larger than the quadrupole-induced dipole term (R^{-7}).

The values of molecular properties used to construct the entries in the third column of Table II.1 were taken from Ref. 15. They are:

μ = -1.1249 a.u. $\qquad$ θ_{yy} = -0.1481 a.u.

θ_{xx} = 0.1773 a.u. $\qquad$ θ_{zz} = -0.0292 a.u.

An experimental dipole polarizability (1.397 a.u.) was used for helium.[9]

III. EFFECT OF ELECTRON CORRELATION

A. Introduction

In the previous chapter we discussed a Hartree-Fock (HF) interaction potential for the $H_2CO(^1A_1)$-$He(^1S)$ system. It is known that the HF method describes only the average interaction between electrons of colliding molecules.[43] Hence for neutral-neutral interactions, the HF method cannot provide an accurate description of the interaction energy in regions where the dispersion interaction plays an important role, since the dispersion interaction arises from the instantaneous mutual response of one molecule to another.[4] Therefore, a correlated calculation is required to yield this contribution to the interaction energy.[4,20] Because accurate scattering cross sections at very low energies are sought for the H_2CO-He system,[13,34b,35] it is important to determine the correlation correction to the HF potential.

It is useful to divide the H_2CO-He interaction potential into three parts--a highly anisotropic repulsive region at small internuclear separations, a region containing the energy minimum at intermediate distances, and a long-range region. The dominating forces in these regions have different physical origins which dictate the use of selected methods for each. Since electron correlation is only a small fraction of the interaction energy at short range (where closed-shell repulsive forces dominate), the potential energy surface in this region is believed to be well described by our previous HF results.[19] In the non-overlap region, perturbation theory estimates show that the dispersion interaction is dominant and that induction contributions (obtainable in the HF approximation) are negligible. Little is known a priori about

the region near the minimum. Since the HF well depth is quite small (~3°K), it is clear that the CI contribution will significantly alter the potential in this region. Therefore, CI calculations are needed to complete the interaction potential for the H_2CO-He system.

Since only small van der Waals attractions arise from dispersion forces, special care must be given to the type of CI calculation performed. Of course, one would like to determine the correlation contribution to the interaction energy from a full CI claculation but that is at present economically unfeasible for most systems. Extensive work on the He_2 system,[3,23,31] which similarly has a small van der Waals minimum, guides our approach to this problem. By carefully choosing configurations for the He_2 system, the dispersion energy was calculated directly (Di-CI).[3,23,31] The main advantage of this method is that the error due to lack of completeness of the basis set (superposition error) is eliminated.[23] However, it does not take into account change in intramolecular correlation of each molecule with internuclear distance.[23,31] Since the change in intramolecular correlation increases with decreasing intermolecular distance, this method overestimates the well depth. As shown by Liu and McLean,[23] the intermolecular and the intramolecular correlations are <u>not</u> additive, thus one cannot add the dispersion energy and the intramolecular correlation to obtain the total CI contribution. To include intramolecular correlation, a CI calculation may be performed which includes all single and double excitations from the HF reference state (S+D CI). Such a computation approximates the total CI energy including dispersion and intramolecular correlation energy. It also includes the superposition error, however,

which generally leads to an artificial increase in well depth. For He_2 a full CI was carried out yielding a well depth of -10.7°K[23b] that is bracketed by the DI-CI value (-12.1°K)[23a] and the S+D CI limit result (-9.3°K).[23a] Unfortunately, as of this writing, there is no basis upon which to presume that this bracketing will hold rigorously for other systems. However, it does show that interaction energies obtained by the various methods are roughly equal. For the larger H_2CO-He system, it is economically feasible to perform only Di-CI and S+D CI calculations.

B. Description of Calculation

To obtain the CI energy, we initially chose to calculate the dispersion energy by the following procedure (Di-CI): (a) compute the HF energy of the system, (b) localize the occupied orbitals,[38] (c) generate configurations that include single and double excitations corresponding to removal of one electron from a H_2CO orbital and one electron from the He orbital, and (d) place the excited electrons into all possible spin and symmetry allowed combinations of HF virtual orbitals.[41] (In all Di-CI calculations, the two lowest orbitals, which correspond to O and C 1s cores, are frozen, i.e., no excitations are permitted.) By calculating the dispersion energy in this manner, no superposition error arises. Using this method at R = 8 and 11 a.u. for both $\theta = 0°$ (O-atom end) and 180° (C-atom end) yields an interaction at the C-atom end that is twice as attractive as that at the O-atom end; see Table III.1. This finding is contrary to what one would expect from HF results where, for fixed R, the interaction at the C-atom end was more repulsive than that at the O-atom end. To verify these values, S+D CI calculations were performed[42] at the same geometries, again holding the lowest two

orbitals fixed. The S+D CI interaction energies were in close accord with Di-CI values. As in the He_2 study,[23] the Di-CI procedure yields a larger well depth than the S+D CI method.

In the HF H_2CO-He study, a very large basis set (basis B) was used to reduce the superposition error. Since the expense of using basis B for the two types of CI calculations described above is presently prohibitive, basis A was reexamined. At R = 8 a.u. and $\theta = 0°$, the superposition error is at most 7°K. Since Di-CI and S+D CI computations are in reasonable agreement using basis A, we feel that the superposition error is likely not larger than 7°K for the geometries considered here. For these reasons, it is felt that basis set A should provide an adequate description of the well and long-range regions and, therefore, is used for the remainder of the calculations.

Although the Di-CI and S+D CI methods yield comparable results, the available S+D CI computer code is faster and, therefore, was the one used for the bulk of the calculations. CI computations were performed at 14 geometries: $\theta = 0°$ and 180° for R = 5, 7, 8 and 11 a.u.; $\theta = 90°$, $\phi = 0°$ (plane of H_2CO) for R = 5, 8 and 11 a.u.; and $\theta = 90°$, $\phi = 90°$ (bisector plane) for R = 5, 8 and 11 a.u. The number of configurations included in the CI wavefunctions depends, of course, on the molecular point group. As discussed elsewhere,[30] each configuration is a pure spin eigenfunction with S = 0. The geometries $\theta = 0°$ and 180° correspond to C_{2v} symmetry (19452 configurations in the S+D CI), $\theta = 90°$, $\phi = 0°$ corresponds to C_s symmetry (37779 configurations) and $\theta = 90°$, $\phi = 90°$ also corresponds to C_s symmetry (34419 configurations), but a different plane of symmetry is involved.

C. Results and Discussion

Correlation energies are given in Table III.1. These values do not include the HF interaction energy and thus must be added to the HF results to get the complete interaction potential. Because of the limited information available for $\theta = 90°$, no correlation contribution to the ϕ dependence can be ascertained.

To facilitate the use of the energy surface in scattering calculations, the correlation contribution is expanded in spherical harmonics. Following Eq. (II.1) the angular dependence of the correlation contribution is expressed in the form

$$V(R,\theta) = v_{00}(R) + v_{10}(R)\cos\theta + \frac{1}{2} v_{20}(R)(3\cos^2\theta - 1) \quad (1)$$

Inverting Eq. (1) gives

$$v_{00}(R) = \frac{V(R,0°) + V(R,180°) + 4V(R,90°)}{6} \quad (2)$$

$$v_{10}(R) = \frac{V(R,0°) - V(R,180°)}{2} \quad (3)$$

and

$$v_{20}(R) = \frac{V(R,0°) + V(R,180°) - 2V(R,90°)}{3} \quad . \quad (4)$$

From Eqs. (1) through (4), the correlation contribution can be interpolated for all desired values of R and θ. The potentials $V(R,\theta)$ have been fit to the radial function

$$V(R,\theta) = Ae^{-BR} - CR^{-6} \quad , \quad (5)$$

where A, B and C for $\theta = 0°$, 90° and 180° are given in Table III.2.

Table III.1. Correlation energies (E_{CI}-E_{HF}) for H_2CO-He.*

R(a.u.)	θ φ	0° 0°	90° 0°	90° 90°	180° 0°
5		-0.000891	-0.000737	-0.000709	-0.002247
		-281.4	-232.7	-223.9	-709.6
7		-0.000171	---	---	-0.000294
		-54.0	---	---	-92.8
8		-0.000064	-0.000040	-0.000026	-0.000115
		-20.2	-12.6	-8.2	-36.3
		(-22.9)**			(-41.9)
11		-0.000005	-0.000001	-0.000001	-0.000009
		-1.6	-0.3	-0.3	-2.8
		(-2.9)			(-4.9)

*Order of entries in the table: energy in a.u. and °K, where $1°K = 3.1668\times10^{-6}$ a.u.

**Energies (°K) in parenthesis are from the Di-CI calculation.

*Table III.2. Parameters for the correlation interaction.**

θ	A**	B	C**
0°	-1.30529 (4)	0.80863	8.19754 (5)
90°	-5.58237 (4)	1.11606	2.08846 (5)
180°	-8.00165 (4)	1.01991	3.46152 (6)

*Distance units are a.u. and energy units are °K.

**Values in parenthesis are powers of 10.

Contour plots of the HF and CI interaction energies in the plane of the H_2CO (ϕ = 0°) and the bisector plane (ϕ = 90°) are given in Fig. 3.1. As expected, the strongly repulsive region is virtually unchanged by including electron correlation. The correlation contribution increases the well depth from 3°K in the HF surface to 35-40°K and shifts the minimum inward from 9 a.u. to 7.5 a.u.

Based on the close agreement of the Di-CI and S+D Ci calculations in the well region (R = 8 a.u.), the final CI interaction energies are believed reliable to ~20%.

D. Summary

A CI calculation has been performed to ascertain the role of electron correlation on the interaction potential between a rigid formaldehyde molecule and a helium atom. Efforts were concentrated on the region of the energy minimum and at large intermolecular distances where correlation effects are expected to have their largest effect.

Two types of CI calculations were carried out. In one method (Di-CI), the dispersion energy was calculated directly by judicious selection of configurations. In the second procedure (S+D CI), the interaction energy was determined from a CI wavefunction built from inclusion of all single and double excitations from a HF reference state. Interaction energies obtained by the two procedures were in reasonable agreement. It is noted that the Di-CI method yields a somewhat larger well depth than the S+D CI procedure as anticipated from previous He_2 studies.[23] CI interaction energies in the vicinity of the minimum have an estimated uncertainty of 20%.

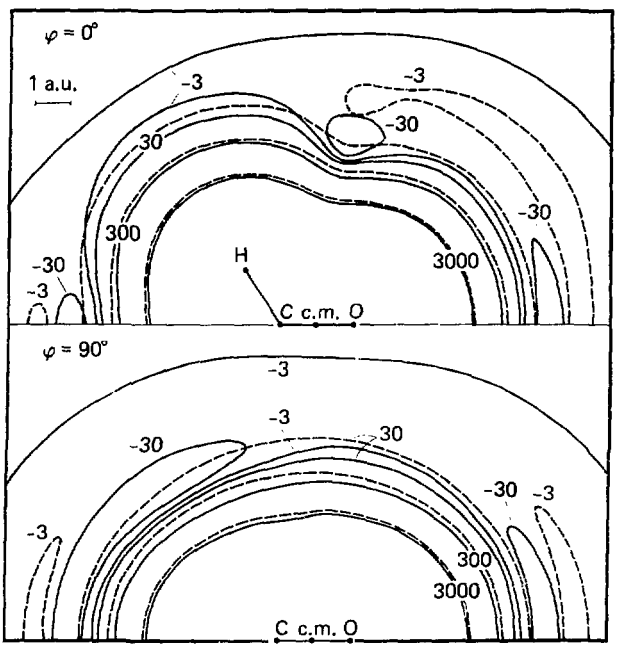

XBL 758-6878

Fig. 3.1. Contour plots of the interaction potential for He incident in the plane of H_2CO ($\phi = 0°$) and He incident in the bisector plane ($\phi = 90°$). —— *Ci interaction* potential. ---- HF interaction potential. Energies in °K. c.m. denotes center of mass.

To facilitate scattering studies, the CI interaction energies were fit to a spherical harmonic expansion. Three terms were used to describe the θ dependence; no significant out-of-(H_2CO) plane dependence ϕ was obtained. The effect of correlation on the well region is to deepen the well from ~3°K to 35-40°K and to shift the minimum inward from a H_2CO-He center of mass separation of 9 to 7.5 a.u.

IV. DETERMINATION OF CROSS SECTIONS

A. Introduction

In this chapter an Arthurs and Dalgarno type coupled channel (CC) formalism is developed for the scattering of an asymmetric top by an atom. With the interaction potential described in Chapters II and III, the CC equations are integrated to determine the rotational cross sections of ortho H_2CO.

B. Asymmetric Top

Before treating the scattering of an asymmetric top by an atom, the properties of the asymmetric top wavefunctions will be briefly summarized. An excellent detailed discussion is given by Davydov.[6]

It is convenient to define two coordinate systems: (1) a space fixed (SF) frame denoted by primes and (2) a body fixed (BF) frame (unprimed) which is attached to the center mass of the top. The BF axes are taken to be coincident with the principal axes of the top. The orientation of the BF axes with respect to the SF axes is given by the three Euler angles ($\alpha\beta\gamma$).[28]

The rotational Hamiltonian of the top is

$$\mathcal{H} = \frac{1}{2}\left(\frac{J_x^2}{I_x} + \frac{J_y^2}{I_x} + \frac{J_z^2}{I_z}\right) \tag{1}$$

$$= AJ^2 + (B - A)\, J_y^2 + (C - A)\, J_z^2 \quad . \tag{2}$$

Here J^2 is the square of the angular momentum operator J, J_i ($i = x,y,z$) are the components of J along the BF axes, I_i are the principal moments of inertia, and $A = \frac{1}{2I_x}$, $B = \frac{1}{2I_y}$ and $C = \frac{1}{2I_z}$ are the rotational

constants. To solve the Schroedinger equation for the Hamiltonian in (2) it is convenient to expand the asymmetric top wavefunction in a basis set of symmetric top (where $I_x = I_y$) wavefunctions, ψ_{jm_jk}. The asymmetric top wavefunction is, therefore, expanded as

$$\phi_\tau^{jm_j}(\alpha\beta\gamma) = \sum_{k=-j}^{j} a_{k\tau}^{j} \psi_{jm_jk}(\alpha\beta\gamma) \tag{3}$$

where

$$\psi_{jm_jk}(\alpha\beta\gamma) = \sqrt{\frac{2j+1}{8\pi^2}}\, D_{m_jk}^{j*}(\alpha\beta\gamma) \tag{4}$$

Here $D_{m_jk}^{j}(\alpha\beta\gamma)$ is an element of the rotation matrix;[28] the $a_{k\tau}^{j}$ are expansion coefficients (to be determined); $j(j+1)\hbar^2$, $m_j\hbar$ ($|m_j| \leq j$), and $k\hbar$ ($|k| \leq j$) are the eigenvalues of J^2, $J_{z'}$ (SF projection), and J_z (BF projection) respectively; and τ labels the asymmetric top eigenfunctions (see below). Note that J^2 and $J_{z'}$ are conserved for both symmetric and asymmetric tops while J_z is conserved only for the <u>symmetric</u> top. The fact that J_z is not conserved results in mixing of the $(2j+1)$ different values of k corresponding to a given (j, m_j) to form $(2j+1)$ states of the asymmetric top. These asymmetric top states are labeled by an index τ as indicated above.

Substitution of (3) into the Schroedinger equation leads to

$$\sum_k a_{k\tau}^{j} \left\{ \langle \psi_{jm_jk'} | \mathcal{H} | \psi_{jm_jk} \rangle - \varepsilon_{j\tau}\delta_{k'k} \right\} = 0 \tag{5}$$

for $(2j+1)$ values of τ. The matrix elements of $\mathcal{H}$ over the symmetric top wavefunctions can be found in Davydov.[6]

The $(2j + 1)$ equations given by (5) can be simplified by employing the symmetry properties of the Hamiltonian. The Hamiltonian is invariant under the group of the following four coordinate transformations: (1) identity transformation, (2) $x \rightarrow -x$, (3) $y \rightarrow -y$ and (4) $z \rightarrow -z$. These transformations form a representation of the Klein Four Group which has four one-dimensional irreducible representations. By transforming the basis of symmetric top wavefunctions to a set of symmetry adapted functions, which transform according to the irreducible representations of the Four Group, the Hamiltonian matrix (see Eq. (5)) becomes block diagonal, thus decoupling the system of Eqs. (5) into four smaller systems. The four classes of symmetry adapted functions, χ, are

$$\chi_{ks}^{odd} = \frac{1}{\sqrt{2}}\left[\psi_{jm_j k} + (-)^s \psi_{jm_j -k}\right]; \quad k \text{ odd}, \; s = 0 \text{ or } 1, \qquad (6a,b)$$

$$\chi_{ks}^{even} = \frac{1}{\sqrt{2(1 + \delta_{ok})}}\left[\psi_{jm_j k} + (-)^s \psi_{jm_j -k}\right] ; \; k \text{ even}, \; s = 0 \text{ or } 1. \qquad (6c,d)$$

Note that there are four types of functions (k is odd or even and $s = 0$ or 1), each of which transforms according to a different irreducible representation. The expansion (3) can now be restricted to sums over a single class of symmetry adapted functions,

$$\phi_\tau^{jm_j} = \sum_{\substack{k=0 \text{ or } 1 \\ \text{even or odd } k}} b_{k\tau}^{j} \chi_{ks}$$

where the state index τ now also implies odd or even values of k and a value of s (0 or 1). The system of Eqs. (5), therefore, becomes four smaller systems of the type

$$\sum_{\substack{k=0 \text{ or } 1 \\ \text{odd or} \\ \text{even } k}} b^{j}_{k\tau}\{(\chi_{k's}|\mathcal{H}|\chi_{ks}) - \varepsilon_{j\tau}\delta_{k'k}\} = 0 \quad . \tag{7}$$

These sets of equations can be solved by standard techniques in linear algebra to yield the eigenvalues $\varepsilon_{j\tau}$ and expansion coefficients $b^{j}_{k\tau}$ of the asymmetric top.

The group described previously does not represent all the symmetry properties of the asymmetric top Hamiltonian. The Hamiltonian also has inversion symmetry (simultaneous inversion of the x, y and z coordinates), thus the full group of the top is $D_{2h} = D_2 \otimes i$. (D_2 is a realization of the Four Group and i represents the inversion group.) In Section III this additional symmetry will be used to simplify the coupled channel scattering equations. For reference the inversion parity of $\phi_\tau^{jm_j}$ is given by

$$F\phi_\tau^{jm_j} = (-)^{j+k+s}\,\phi_\tau^{jm_j} \tag{8}$$

where F is the inversion operator. Hence the symmetry adapted functions of (6) are automatically symmetry adapted functions of the larger group D_{2h}.

For the case of H_2CO there is the additional symmetry of interchanging the identical H nuclei resulting in ortho (symmetric) and para (antisymmetric) couplings of nuclear spins. Since there is no interaction that couples nuclear spin states during collisions with He, ortho and para H_2CO can be treated as separate species. The astrophysical observations of interest in this study are of ortho H_2CO; therefore, only these states need be included in the scattering

calculations. Since the H nuclei are Fermions, the total wavefunction must be antisymmetric under their interchange. The nuclear wavefunction is symmetric, and therefore the rotational wavefunctions must be antisymmetric. Letting P be the operator that interchanges H nuclei then

$$P\phi_{\tau}^{jm_j} = (-)^k \phi_{\tau}^{jm_j} \tag{9}$$

where again τ implies odd or even values of k. Since $\phi_{\tau}^{jm_j}$ must be antisymmetric for ortho H_2CO, Eq. (9) shows that only states with k odd (functions given by (6a,b)) are required in this study.

Using the rotational constants of Oka[26] (A = 38835 MHz, B = 43003 MHz, and C = 282029 MHz) to evaluate the Hamiltonian matrix elements, the energy levels of ortho H_2CO were obtained from the solution of (7). These energy levels accompanied by two labeling schemes are given in Fig. 4.1. For the lower (upper) state of each doublet s is 1 (0).

C. Theory of Atom-Molecule Scattering

In this section, the Arthurs and Dalgarno[1] (AD) coupled channel or close coupling (CC) formulation is presented for the case of scattering of an asymmetric top by an atom. For simplicity the atom is assumed spherical (in a ^1S state) and the top is also taken to be in a singlet state so that the problems associated with the coupling of spin angular momentum can be neglected. Low kinetic energies will be considered; therefore, vibrational and electronic excitation is not possible.

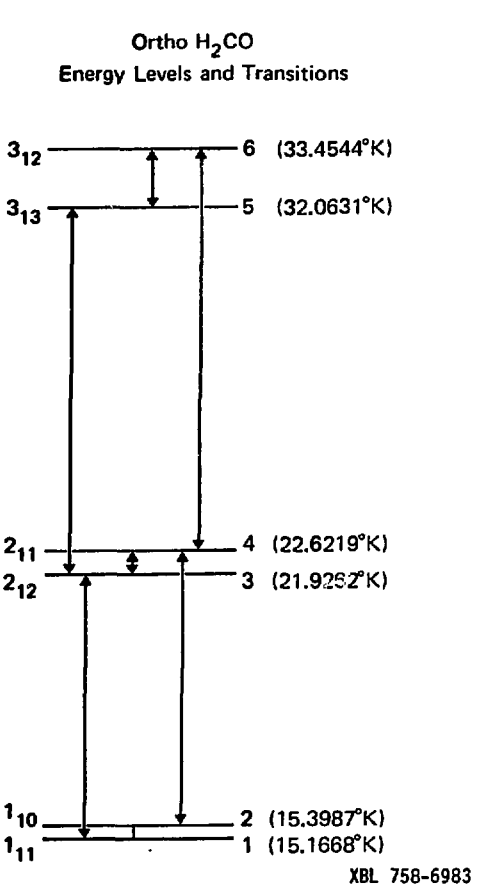

Fig. 4.1. Energy level diagram for ortho H_2CO with the dipole allowed transitions designated by arrows.

The Hamiltonian of the total system (top plus atom) in center of mass coordinates is

$$\mathcal{H} = (-\hbar^2/2\mu)\,\nabla^2_{\vec{r}} + \mathcal{H}_{int}(\hat{R}') + V(\vec{r},\hat{R}') \quad , \tag{10}$$

where the terms from left to right are the kinetic energy operator for the relative motion of the top and the atom, the rotational Hamiltonian (Eq. (2)) of the top, and the intermolecular potential. Here μ is the reduced mass of the total system, $\vec{r} \equiv (r,\theta',\phi')$ is the position of the atom in a space fixed (SF) frame and $\hat{R}' \equiv (\alpha\beta\gamma)$ is the orientation of the top in the SF frame.

To solve the Schoedinger equation

$$(\mathcal{H} - E_{tot})\,\Psi = 0 \tag{11}$$

an expansion technique is used. The total angular momentum $\vec{J}$ and its SF z' projection $J_{z'} = M$ are conserved in this system. AD found it convenient to couple the rotational angular momentum ($\vec{j}$) of the top and the orbital angular momentum ($\vec{\ell}$) of the colliding system together to form eigenfunctions of $\vec{J}$ and $J_{z'}$. Following AD the radial and angular dependences are separated and the wavefunction is written as

$$\Psi^{JM}_{j\ell\tau}(\vec{r},\hat{R}') = \sum_{j'\ell'\tau'} \frac{1}{r}\, u^{J}_{j'\ell'\tau'\leftarrow j\ell\tau}(r) \times Y^{JM}_{j'\ell'\tau'}(\hat{r}',\hat{R}') \tag{12}$$

where

$$y^{JM}_{j\ell\tau}(\hat{r}',\hat{R}') = \sum_{m_j=-j}^{j} \sum_{m_\ell=-\ell}^{\ell} C(j\ell J; m_j m_\ell M) \times Y_{\ell m_\ell}(\hat{r}')\, \phi_\tau^{j m_j}(\hat{R}') \quad . \tag{13}$$

Here, $C(j\ell J; m_j m_\ell M)$ is a Clebsch-Gordan coefficient,[28] $Y_{\ell m_\ell}(\hat{r}')$ is a spherical harmonic describing the relative angular momentum of the colliding system and $\phi_\tau^{j m_j}(\hat{R}')$ is the asymmetric top function given by Eq. (3). Substituting Eqs. (10), (12) and (13) into (11), multiplying on the left by $y^{JM*}_{j''\ell''\tau''}$, integrating over $\hat{r}'$ and $\hat{R}'$, and making use of orthonormality relations,[28] yields the CC equations

$$\left[d^2/dr^2 - \ell'(\ell'+1)/r^2 + k^2_{j'\tau'}\right] u^J_{j'\ell'\tau',j\ell\tau}(r) = (2\mu/\hbar^2) \sum_{j''} \sum_{\ell''} \sum_{\tau''} \langle j'\ell'\tau'|V|j''\ell''\tau''\rangle\, u^J_{j''\ell''\tau'',j\ell\tau}(r) \tag{14}$$

where

$$k^2_{j'\tau'} = 2\mu(E_{tot} - \varepsilon_{j'\tau'})/\hbar^2 \quad . \tag{15}$$

The coupling matrix elements are defined by

$$\langle j'\ell'\tau'|V|j''\ell''\tau''\rangle = \iint d\hat{R}'\, d\hat{r}'\, y^{JM*}_{j'\ell'\tau'}(\hat{r}',\hat{R}') \times V(\vec{r},\hat{R}')\, y^{JM}_{j''\ell''\tau''}(\hat{r}',\hat{R}') \tag{16}$$

and are independent of M. For an asymmetric top and an atom the interaction potential can be expressed as (see Eq. II.1)

$$V(\vec{r},\hat{R}') = \sum_{\lambda=0}^{\infty} \sum_{\nu=-\lambda}^{\lambda} (4\pi/2\lambda+1)^{1/2}\, v_{\lambda\nu}(r)\, Y_{\lambda\nu}(\theta,\phi) \tag{17}$$

where θ and ϕ are the angles that define the position of the atom with respect to the top. Since (θ,ϕ) are not the angles used previously and integration over angles is required by (16), the group representation property[39] is used to write $Y_{\lambda\nu}(\theta,\phi)$ as a function of the angles $\hat{r}'$ and $\hat{R}'$. The potential is alternately written as

$$V(\vec{r},\hat{R}') = \sum_{\lambda\nu\nu'} (4\pi/2\lambda+1)^{1/2} \; v_{\lambda\nu}(r)\; Y_{\lambda\nu'}(\hat{R}')\; D^{\lambda}_{\nu',\nu}(\hat{r}') \quad . \tag{18}$$

Substitution of Eqs. (3), (13), and (18) into (16) yields the explicit form of the coupling matrix elements

$$\langle j'\ell'\tau'|V|j''\ell''\tau''\rangle = (-)^{j'+j''-J} \sum_{k'=-j'}^{j'} \sum_{k''=-j''}^{j''} a^{j'}_{k',\tau'} a^{j''}_{k''\tau''} (-)^{k''} \sum_{\lambda} v_{\lambda,k''-k'}(r)$$

$$\times [(2j'+1)(2j''+1)(2\ell'+1)(2\ell''+1)]^{1/2} \begin{pmatrix} \ell' & \ell'' & \lambda \\ 0 & 0 & 0 \end{pmatrix} \begin{pmatrix} j' & j'' & \lambda \\ k' & -k'' & k''-k' \end{pmatrix} \begin{Bmatrix} j' & \ell' & J \\ \ell'' & j'' & \lambda \end{Bmatrix} \tag{19}$$

The $(:::)$ are 3-j symbols and $\{:::\}$ is a 6-j symbol.[29]

Symmetry considerations simplify evaluation of the coupling matrix elements. Conservation of parity requires the coupling matrix elements (19) to vanish unless

$$(-)^{j'+k+s'+\ell'} = (-)^{j''+k''+s''+\ell''} \quad . \tag{20}$$

(Recall from Section *II* that τ implies odd or even values of k and s to be 0 or 1.) Hermiticity of the potential results in

$$\langle j''\ell''\tau''|V|j'\ell'\tau'\rangle = \langle j'\ell'\tau'|V|j''\ell''\tau''\rangle \quad . \tag{21}$$

The boundary condition on the radial function

$$u^J_{j'\ell'\tau'\leftarrow j\ell\tau}(r) \sim \delta_{jj'}\delta_{\ell\ell'}\delta_{\tau\tau'} \exp[-i(k_{j\tau}r - \ell\pi/2)] \tag{22}$$

$$- \left(\frac{k_{j\tau}}{k_{j'\tau'}}\right)^{1/2} S^J_{j'\ell'\tau'\leftarrow j\ell\tau} \exp[i(k_{j\tau}r - \ell\pi/2)]$$

defines the scattering matrix S^J. For the $j'\tau' \leftarrow j\tau$ transition the integral cross section is given by

$$\sigma_{j'\tau'\leftarrow j\tau} = \frac{\pi}{(2j+1)\,k^2_{j\tau}} \sum_{J=0}^{\infty} (2J+1) \sum_{\ell=|J-j|}^{J+j} \sum_{\ell'=|J-j'|}^{J+j'} |T^J_{j'\ell'\tau'\leftarrow j\ell\tau}|^2 \tag{23}$$

where

$$T^J_{j'\ell'\tau'\leftarrow j\ell\tau} = \delta_{jj'}\delta_{\ell\ell'}\delta_{\tau\tau'} - S^J_{j'\ell'\tau'\leftarrow j\ell\tau} \quad . \tag{24}$$

The cross section in Eq. (23) has been obtained by averaging over initial projections m_j and summing over final projections $m_{j'}$. Since the S matrix is unitary the reverse cross sections can be obtained from the reciprocity relation

$$\sigma_{j\tau\leftarrow j'\tau'} = \frac{(2j+1)\,k^2_{j\tau}}{(2j'+1)\,k^2_{j'\tau'}} \sigma_{j'\tau'\leftarrow j\tau} \quad . \tag{25}$$

D. Description of Scattering Calculations

The cross sections for rotational excitation of ortho H_2CO by collision with He are determined by integrating the coupled channel equations (14). In order to carry out the integration it is necessary to specify the total energy of the system E_{tot} (see Eq. (11)), the number of internal H_2CO states, and the integration procedure. For the astrophysical problem Boltzmann averaged rate constants are required (see Section VI), and accordingly 12 values of E_{tot} in the range $20° \leq E_{tot} \leq 95°K$ were chosen. (See Table IV.1 or IV.2 for a list of values.) The sums on the right hand side of the CC equations (14) extend, in principle, over an infinite number of (j,τ,ℓ) combinations. Obviously, this is not computationally feasible so the sums must be restricted, keeping only the important terms. This is done by chosing a basis of internal ortho H_2CO states (j,τ) and then selecting the values of orbital angular momentum ℓ permitted by the triangle inequalities of angular momentum coupling for a given value of J (total angular momentum). For this calculation a basis set of 16 ortho H_2CO states with $1 \leq j \leq 5$ were chosen. This resulted in a maximum of 62 channels ((j,τ,ℓ) combinations) coupled together. At E_{tot}'s less than 50°K there are 4-8 H_2CO states energetically accessible in the asymptotic region. The CC equations were integrated by Gordon's method[17] with the tolerance parameters VMAX, TMAX, TOLLO, TOLHI, CTOL set at 10^{-4} and the parameters STEST and UTEST set at 10^{-3}. The interaction potential (Eq. (17)) is the sum of the Hartree-Fock contribution (Eq. (II.1)) and the correlation contribution (Eq. (III.1)).

E. Results

The elastic cross sections for the six lowest ($j \leq 3$) ortho H_2CO states are given in Table IV.1 and displayed as a function of E_{tot} in Fig. 4.2. The inelastic cross sections are given in Table IV.2. Selected inelastic cross sections are plotted in Fig. 4.3. Reverse transitions were obtained from the reciprocity relation (25).

Resonances occur at ~20.2, 32.7 and 47.7°K in many of the cross section curves. These energies are approximately equal to the internal energies of the $j = 2$, 3 and 4 doublets, respectively.

Table IV.1. Coupled channel elastic cross sections.*

State	E_{tot}(°K)											
	20.1668	25.1668	27.6668	30.1668	32.6668	35.1668	37.6668	40.1668	42.6668	47.6668	70.1668	95.1668
1_{11}	331	235	229	213	345	189	179	170	163	152	115	93
1_{10}	331	257	241	231	418	194	182	174	167	154	115	93
2_{12}	---	267	282	249	430	217	205	197	186	178	122	96
2_{11}	---	308	306	263	414	228	211	204	195	187	124	97
3_{13}	---	---	---	---	1620	289	277	255	244	259	135	103
3_{12}	---	---	---	---	----	253	288	293	281	353	142	106
4_{13}	---	---	---	---	----	---	---	---	---	950	162	112
4_{12}	---	---	---	---	----	---	---	---	---	---	178	116

*Units are $Å^2$.

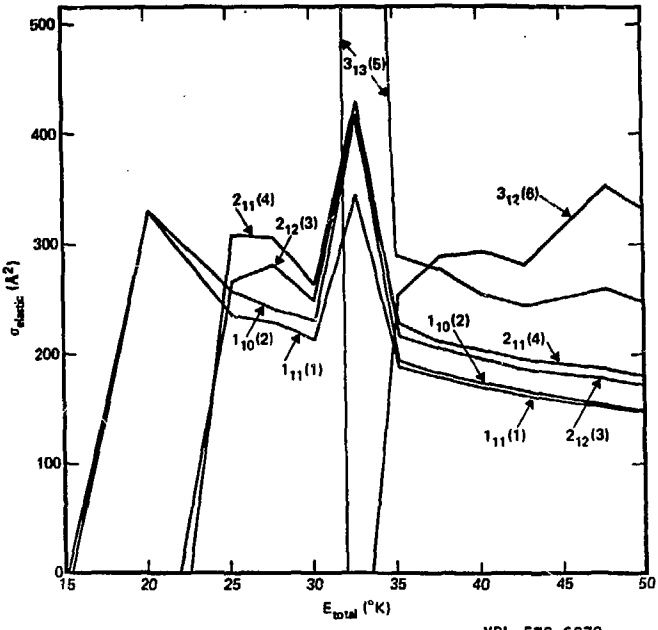

XBL 578-6879

Fig. 4.2. Elastic cross sections.

Table IV.2. Coupled channel inelastic cross sections.*

Transition	E_{tot}(°K) 20.1668	25.1668	27.6668	30.1668	32.6668	35.1668	37.6668	40.1668	42.6668	47.6668	70.1668	95.1668
$1_{11}-1_{10}$	66.0	25.6	17.8	15.1	45.5	12.3	11.5	11.1	10.1	9.5	7.6	6.6
$1_{11}-2_{12}$	----	22.7	23.3	23.3	37.6	20.2	18.1	17.1	16.7	16.1	10.5	8.5
$1_{11}-2_{11}$	----	12.2	11.8	13.9	17.1	11.2	9.5	8.9	8.0	7.7	5.7	5.2
$1_{11}-3_{13}$	----	----	----	----	4.8	4.1	5.4	6.3	6.4	8.0	5.4	4.6
$1_{11}-3_{12}$	----	----	----	----	----	0.3	0.6	0.8	1.2	1.6	0.9	1.3
$1_{11}-4_{14}$	----	----	----	----	----	----	---	---	---	3.0	3.5	3.8
$1_{11}-4_{13}$	----	----	----	----	----	----	---	---	---	---	0.9	1.2
$1_{10}-2_{12}$	----	13.4	13.8	15.4	33.1	11.5	9.9	9.7	9.2	8.5	6.3	5.4
$1_{10}-2_{11}$	----	14.2	13.3	16.0	34.9	14.3	12.4	11.6	10.3	8.9	8.4	7.8
$1_{10}-3_{13}$	----	----	----	----	2.5	7.6	8.6	7.6	7.2	7.0	4.7	3.4
$1_{10}-3_{12}$	----	----	----	----	----	1.6	2.4	2.6	3.7	4.7	4.5	4.3
$1_{10}-4_{14}$	----	----	----	----	----	----	---	---	---	3.0	2.5	2.2
$1_{10}-4_{13}$	----	----	----	----	----	----	---	---	---	---	0.6	0.7
$2_{12}-2_{11}$	----	24.8	19.4	19.9	92.4	13.1	10.4	8.4	7.1	5.5	3.5	2.8
$2_{12}-3_{13}$	----	----	----	----	10.8	11.9	13.3	13.3	12.9	20.0	11.6	11.1
$2_{12}-3_{12}$	----	----	----	----	----	2.1	3.3	3.7	3.7	9.5	3.4	3.1
$2_{12}-4_{14}$	----	----	----	----	----	----	---	---	---	4.2	3.0	3.3
$2_{12}-4_{13}$	----	----	----	----	----	----	---	---	---	---	1.1	1.3
$2_{11}-3_{13}$	----	----	----	----	7.6	7.1	7.9	6.6	7.3	12.3	3.7	2.8
$2_{11}-3_{12}$	----	----	----	----	----	8.2	11.5	12.1	10.4	20.2	9.5	8.2
$2_{11}-4_{14}$	----	----	----	----	----	----	----	----	----	4.2	3.9	3.4
$2_{11}-4_{13}$	----	----	----	----	----	----	----	----	----	---	3.3	3.6
$3_{13}-3_{12}$	----	----	----	----	----	9.6	10.2	8.8	9.2	25.0	2.8	2.1
$3_{13}-4_{14}$	----	----	----	----	----	----	---	----	----	14.1	11.9	10.7
$3_{13}-4_{13}$	----	----	----	----	----	----	---	----	----	----	2.4	2.4
$3_{12}-4_{14}$	----	----	----	----	----	----	---	----	----	12.7	2.6	1.9
$3_{12}-4_{13}$	----	----	----	----	----	----	---	----	----	----	10.0	9.6
$4_{14}-4_{13}$	----	----	----	----	----	----	---	----	----	----	2.7	1.8

*Units are $Å^2$.

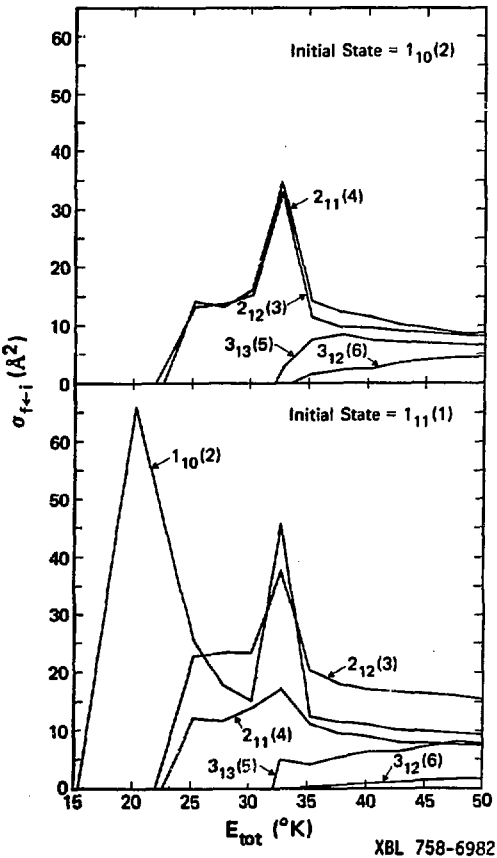

Fig. 4.3. Inelastic cross sections for initial states 1_{11} and 1_{10}.

V. COOLING OF INTERSTELLAR FORMALDEHYDE

In order to test the collisional pump as a mechanism for cooling of interstellar H_2CO, the rotational cross sections given in Chapter IV will be used to determine excitation temperatures. For simplicity we will assume that the only processes of importance are dipole radiation and collisions. Higher moment transition probabilities are several orders of magnitude smaller than dipole ones, and hence they are neglected here.[14] It will also be assumed that the interstellar medium is rare enough to neglect radiative trapping.[13]

Astrophysical observations indicate that the 6 cm (j = 1) and 2 cm (j = 2) doublets of ortho H_2CO are cooled, i.e., the excitation temperatures T_{exc} between states 1 and 2 (see Fig. 4.1) and between states 3 and 4 are less than either the isotropic background temperature ($T_{iso} \simeq 2.7°K$) or the kinetic temperature ($10° \leq T_k \leq 20°K$). The excitation temperature is defined by assuming a Boltzmann distribution for the populations of two internal states, viz,

$$\frac{n_i}{n_j} = \frac{g_i \exp(-E_i/k_B T_{exc})}{g_j \exp(-E_j/k_B T_{exc})} \tag{1}$$

where n_i = population of the i^{th} internal state

g_i = degeneracy of the i^{th} internal state

E_i = energy of the i^{th} internal state

k_B = Boltzmann's constant.

Then if the populations of two states are known the excitation temperature characterizing them can be determined.

The populations are determined by solving the equations of statistical equilibrium,[5]

$$\frac{dn_i}{dt} = \sum_{j \neq i} \{A_{ji} + B_{ji}\rho(\nu_{ij}) + [He]\, k_{ji}\}\, n_j - \left\{\sum_{j \neq i} A_{ij} + B_{ij}\rho(\nu_{ij}) + [He]\, k_{ij}\right\} n_i = 0 \qquad (2)$$

where A_{ij} is the Einstein coefficient for spontaneous dipole emission from state i to state J ($E_i > E_j$) (Table V.1), B_{ij} is the Einstein coefficient for induced dipole emission and absorption (Table V.2), $\rho(\nu_{ij})$ is the energy distribution of radiation at the isotropic background temperature (2.7°K), $\nu_{ij} = |E_i - E_j|/h$ and [He] is the helium concentration.[14] Here k_{ij} is the collisional rate constant for transition from state i to state j obtained by Boltzmann averaging the cross sections (as determined in Chapter IV) as follows (Table V.3):

$$k_{ij}(T_k) = \left(\frac{8}{\pi\mu(k_B T_k)^3}\right)^{1/2} \int_0^\infty E\, \sigma_{j \leftarrow i}(E)\, e^{-E/k_B T_k}\, dE \qquad (3)$$

where $E = E_{tot} - E_i$ is the relative translational energy.

Assuming a kinetic temperature and a helium concentration, the system of equations defined by Eq. (2) is solved for the populations. Excitation temperatures are then calculated using Eq. (1). In the limit [He] → 0, i.e., radiation processes only (no collisions), all the excitation temperatures reduce to T_{iso}. As [He] → ∞ the collisional processes become dominant and all $T_{exc} \rightarrow T_k$. At helium concentrations between these limits T_{exc} lower than both T_{iso} and T_k can occur.

Table V.1. Spontaneous emission coefficients matrix A.*

Initial State	Final State 1_{11}	1_{10}	2_{12}	2_{11}	3_{13}	3_{12}	4_{13}	4_{12}
1_{11}	---	---	---	---	---	---	---	---
1_{10}	0.4	---	---	---	---	---	---	---
2_{12}	5261.2	---	---	---	---	---	---	---
2_{11}	---	6420.2	3.2	---	---	---	---	---
3_{13}	---	---	22739.4	---	---	---	---	---
3_{12}	---	---	---	27504.1	11.9	---	---	---
4_{13}	---	---	---	---	58007.1	---	---	---
4_{12}	---	---	---	---	---	71264.6	35.4	---

*Units of 10^{-8} (molecule -sec)$^{-1}$.

Table V.2. Induced radiation times radiation density matrix B•ρ.*

Initial State	Final State 1_{11}	1_{10}	2_{12}	2_{11}	3_{13}	3_{12}	4_{13}	4_{12}
1_{11}	---	3.9	781.2	---	---	---	---	---
1_{10}	3.9	---	---	791.7	---	---	---	---
2_{12}	468.7	---	---	10.8	754.6	---	---	---
2_{11}	---	475.0	10.8	---	---	709.7	---	---
3_{13}	---	---	539.0	---	---	18.2	509.4	---
3_{12}	---	---	---	506.9	18.2	---	---	438.0
4_{13}	---	---	---	---	396.2	---	---	26.0
4_{12}	---	---	---	---	---	340.7	26.0	---

*Units of 10^{-8} (molecule -sec)$^{-1}$.

Table V.3. Rate constants* at T_k = 15°K.

Initial State	Final State							
	$^1_{11}$	$^1_{10}$	$^2_{12}$	$^2_{11}$	$^3_{13}$	$^3_{12}$	$^4_{14}$	$^4_{13}$
$^1_{11}$	---	5.5	5.0	2.5	1.3	0.2	0.4	0.1
$^1_{10}$	5.6	---	3.1	3.4	1.3	0.8	0.3	0.0
$^2_{12}$	4.7	2.8	---	3.9	3.8	1.3	0.6	0.1
$^2_{11}$	2.5	3.3	4.1	---	2.0	3.4	0.6	0.3
$^3_{13}$	1.7	1.7	5.3	2.7	---	3.4	2.8	0.3
$^3_{12}$	0.3	1.1	2.1	4.9	3.8	---	1.5	1.4
$^4_{14}$	1.0	0.8	1.6	1.7	5.4	2.6	---	0.5
$^4_{13}$	0.2	0.1	0.3	0.9	0.7	2.9	0.6	---

*In units of 10^{-11} cc/molecule-sec.

Figure 5.1 displays cooling curves (T_{exc} vs [He]) at T_k = 5, 10, 15 and 20°K. Cooling of both the 6 cm (T_{12}) and 2 cm (T_{34}) doublets is seen to occur at helium concentrations between 10^2 and 10^5 cm^{-3} for kinetic temperatures between 10 and 20°K but not for 5°K. The two remaining curves, T_{13} and T_{24}, are excitation temperatures for pairs of states where dipole radiation is allowed.

Having established that the 6 cm and 2 cm doublets of H_2CO are cooled by a collisional pump, the question of the relative importance of the various transitions remains to be fully elucidated. By varying the number of states used in the equations of statistical equilibrium (limit of summation in Eq. (2)), the effect of the different j doublets on the cooling can be assessed (see Fig. 5.2). Neglecting the j = 4 levels caused less than 0.2°K changes in the effective temperatures for He concentrations at which cooling occurs. Omission of the j = 3 levels, however, resulted in <u>no</u> cooling. Thus the j = 3 ortho doublet plays a fundamental role in the cooling of H_2CO. At low He concentrations ($\lesssim 10^5$ cm^{-3}) radiative contributions are found to dominate collisional dipole-allowed transitions so that rate constants k_{12}, k_{13}, k_{24}, k_{34}, k_{35}, k_{46} and k_{56} are of minor importance. Ratios of dipole forbidden transitions, e.g., k_{25}/k_{16}, are the indicators of cooling. The large ratio of $k_{25}/k_{16} \approx 6$ (Table V.3) implies that transitions from the j = 1 to the j = 3 doublets are the primary components of the cooling mechanism.

For collisions of the isotopic homologue $H_2{}^{13}CO$ the Born-Oppenheimer interaction potential is the same as before and all differences are contained in the dynamical treatment. They involve small changes in

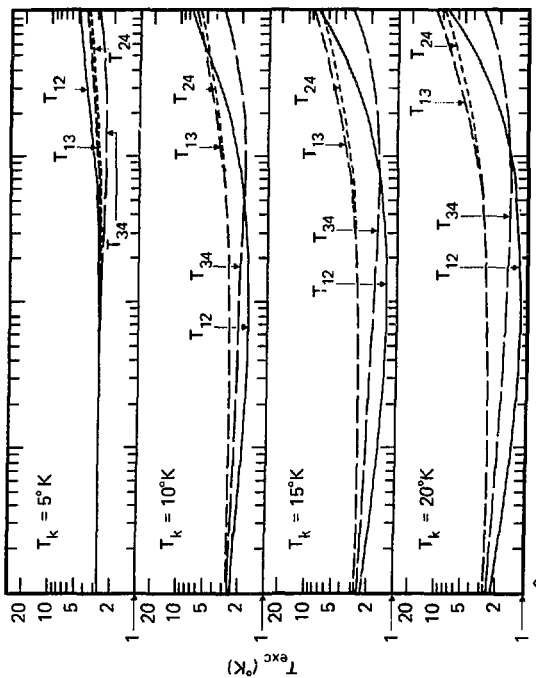

XBL 758-6881

Fig. 5.1. Excitation temperatures as a function of He density at selected kinetic temperatures.

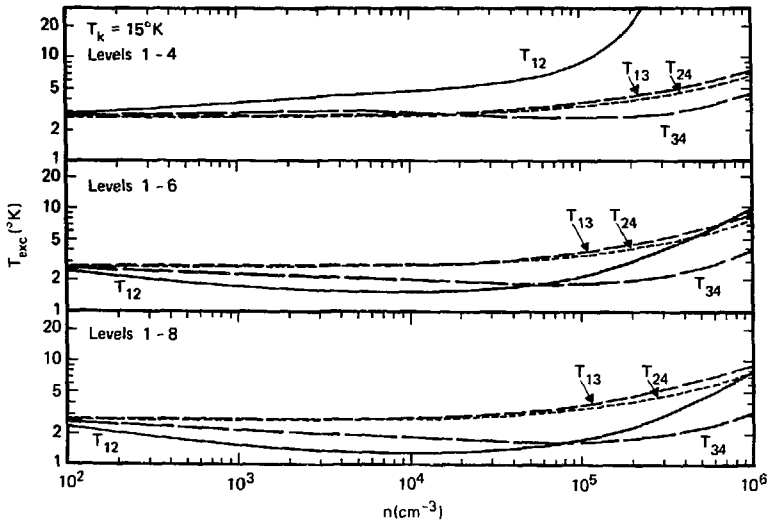

XBL 758-6880

Fig. 5.2. Excitation temperatures as a function of He density with various numbers of internal states included in the equations of statistical equilibrium.

the center of mass of H_2CO, the reduced mass of the total system and the energy level spacing. These differences are expected to have little effect on the scattering cross sections. In agreement with observations, these calculations indicate that the j = 1 doublet of $H_2{}^{13}CO$ is cooled.

By a series of accurate quantum mechanical calculations, the collisional pump is confirmed as a cooling mechanism for the 6 cm (j = 1) and 2 cm (j = 2) doublets of ortho H_2CO. The j = 3 levels are found to be an integral part of the pumping scheme.

ACKNOWLEDGEMENTS

I wish to express my gratitude to Professors William H. Miller and Henry F. Schaefer, III, both of whom have given me guidance during my years as a graduate student at the University of California in Berkeley. In addition, I would like to express my sincerest thanks to Dr. William A. Lester, Jr. at the IBM Research Laboratory for a very rewarding interaction during the 2 years that we worked together.

While in graduate school I have had rewarding interactions with both Professor Miller and Schaefer's research groups and my research associates at IBM. To these many friends and co-workers I say "thank you". Especially I would like to thank David Yarkony for his continued interest in my work and for critically reading my manuscripts.

This work has been performed under the auspices of the U. S. Energy and Research Development Administration. In addition IBM has provided facilities under a joint study agreement with the Lawrence Berkeley Laboratory.

REFERENCES AND FOOTNOTES

1. A. M. Arthurs, and A. Dalgarno, Proc. Roy. Soc. A256, 540 (1960).
2. S. D. Augustin and W. H. Miller, J. Chem. Phys. 61, 3155 (1974).
3. P. J. Bertoncini and A. C. Wahl, Phys. Rev. Lett. 25, 991 (1970); Chem. Phys. 58, 1259 (1973).
4. A. D. Buckingham, Adv. Chem. Phys. 12, 107 (1967). See also, J. O. Hirschfelder, C. F. Curtiss and R. B. Bird, Molecular Theory of Gases and Liquids (John Wiley & Sons, Inc., NY, 1964) and H. Margenau and N. R. Kestner, Theory of Intermolecular Forces (Pergamon Press, NY, 1971).
5. N. R. Davidson, Statistical Mechanics (McGraw-Hill, Inc, NY, 1962).
6. A. S. Davydov, Quantum Mechanics (Pergamon Press, Oxford, 1965).
7. N. H. Dieter, Ap. J. 183, 449 (1973).
8. F. B. Van Duijneveldt, IBM Research Report RJ 945, December 1971. (Available from: Research Library, IBM Research Laboratory, San Jose, CA 95193).
9. L. Essen, Proc. Phys. Soc. (London) B66, 189 (1953).
10. N. J. Evans, II, Ph. D. Thesis, University of California, Berkeley, (1973).
11. N. J. Evans, II, in preparation.
12. N. J. Evans, II, A. C. Cheung and R. M. Sloanaker, Ap. J. (Letters) 159, L9 (1970).
13. N. J. Evans, II, B. Zuckerman, G. Morris and T. Sato, Astrophys. J. 196, 433 (1975).
14. H. Eyring, J. Walter and G. E. Kimball, Quantum Chemistry (John Wiley and Sons, Inc., NY, 1964).

15. B. J. Garrison, H. F. Schaefer, III and W. A. Lester, Jr., J. Chem. Phys. 61, 3039 (1974).

16. P. L. Goodfriend, F. W. Birss and A. B. F. Duncan, Rev. Mod. Phys. 32, 307 (1960).

17. (a) R. G. Gordon, J. Chem. Phys. 51, 14 (1969); (b) Methods Comput. Phys. 10, 81 (1971); (c) Program 187 Quantum Chemistry Program Exchange (QCPE), Indiana University, Bloomington, IN.

18. S. Green, B. J. Garrison and W. A. Lester, Jr., "Hartree-Fock and Gordon-Kim Interaction Potentials for Scattering of Closed Shell Molecules by Atoms: (H_2CO,He) and (H_2,Li^+)" (to appear).

19. Reviews of HF and CI interaction potentials for scattering are given by: (a) M. Krauss, Ann. Rev. Phys. Chem. 21, 39 (1970); (b) P. R. Certain and L. W. Bruch, in MTP International Review of Science, W. Byers Brown, ed. (University Park Press, Baltimore, 1972), Vol. 1, p. 113; (c) R. D. Levine, in MTP International Review of Science, W. Byers Brown, ed. (University Park Press, Baltimore, 1972), Vol. 1, p. 229; (d) J. N. L. Connor, Ann. Repts. Chem. Soc. 70A, 5 (1973); (e) G. G. Balint-Kurti in Advances in Molecular Beams, K. P. Lawley, ed., to appear); (f) W. A. Lester, Jr., Adv. Quant. Chem. 9, (1975) (to appear).

20. A. M. Lesk, J. Chem. Phys. 59, 44 (1973).

21. (a) W. A. Lester, Jr. and M. Krauss, J. Chem. Phys. 52, 4775 (1970) (b) W. A. Lester, Jr., J. Chem. Phys. 53, 1511 (1970); (c) W. A. Lester, Jr., J. Chem. Phys. 54, 3171 (1971); (d) W. Kutzelnigg, V. Staemmler and K. Hoheisel, Chem. Phys. 1, 27 (1973).

22. M. M. Litvak, Ap. J. (Letters) 160, L133 (1970).

23. (a) B. Liu and A. D. McLean, J. Chem. Phys. 59, 4557 (1973); (b) B. Liu and A. D. McLean, unpublished results.

24. Y. K. Minn and J. M. Greenberg, Astr. and Ap. 22, 13 (1973).

25. T. Oka, Ap. J. (Letters) 160, L69 (1970).

26. T. Oka, J. Phys. Soc. (Japan) 15, 2274 (1960).

27. P. Palmer, B. Zuckerman, D. Buhl and L. E. Snyder, Astrophys. J. 156, L147 (1969).

28. M. E. Rose, Elementary Theory of Angular Momentum (John Wiley & Sons, Inc., NY, 1957).

29. M. Rotenberg, R. Bivins, N. Metropolis and J. K. Wooten, Jr., The 3-j and 6-j Symbols (Technology Press, Cambridge, MA, 1959).

30. B. Roos, Chem. Phys. Lett. 15, 153 (1972).

31. (a) H. F. Schaefer, III, D. R. McLaughlin, F. E. Harris and B. J. Alder, Phys. Rev. Lett. 25, 988 (1970); (b) D. R. McLaughlin and H. F. Schaefer, III, Chem. Phys. Lett. 12, 244 (1971).

32. P. M. Solomon and P. Thaddeus, Bull. AAS 2, 218 (1970) (abstract of paper delivered at 131st meeting of AAS, New York City).

33. K. Takagi and T. Oka, J. Phys. Soc. Japan 18, 1174 (1963).

34. (a) P. Thaddeus, Ann. Rev. Astr. and Ap. 10, 305 (1972); (b) P. Thaddeus, Astrophys. J. 173, 317 (1972).

35. C. H. Townes and A. C. Cheung, Astrophys. J. 157, L103 (1969).

36. Simply stated, the effect of basis functions on one atom assisting basis functions on another center and thereby leading to an incorrect description of the interaction between the two atoms. For a fuller discussion, applied to CI wavefunctions, see Ref. 23a.

37. The helium dipole polarizability obtained using basis set B is 1.300 a.u. See Ref. 9 for an experimental value.

38. Since the one He orbital has A_1 symmetry, only the A_1 occupied orbitals were localized.

39. An example of the group representation property is the spherical harmonic addition formula. For a fuller discussion see J. D. Talman, Special Functions (W. A. Benjamin, Inc., NY, 1968).

40. The computer program IBMOL-version 6 was made available by Dr. E. Clementi.

41. The joint MOLECULAR-ALCHEMY program package incorporates the MOLECULE integral program and the ALCHEMY SCF program. MOLECULE was written by Dr. J. Almlöf of the University of Uppsala, Sweden. The ALCHEMY SCF program was written by Drs. P. S. Bagus and B. Liu of the IBM San Jose Research Laboratory. The interfacing of these programs was performed by Drs. U. Wahlgren (presently at the University of Uppsala) and P. S. Bagus at IBM. For a description of MOLECULE see J. Almlöf, Proceedings of the Second Seminar on Computational Problems in Quantum Chemistry, p. 14, Strassburg, 1972 (Max-Planck Institute, Munich 1973). For a description of the ALCHEMY-SCF program, see: P. S. Bagus, Documentation for ALCHEMY--Energy Expressions for Open Shell Systems, IBM Research Report RJ 1077 (1972). The ALCHEMY quantum chemistry programs were written primarily by P. S. Bagus, B. Liu, A. D. McLean and M. Yoshimine of the Theoretical Chemistry Group at IBM Research in San Jose, CA. Preliminary descriptions of the program are given in: (a) A. D. McLean, Potential Energy Surfaces from ab initio

Computation: Current and Projected Capabilities of the ALCHEMY Computer Program, Proceedings of the Conference on Potential Energy Surfaces in Chemistry held at the University of California, Santa Cruz, August 1970; and (b) P. S. Bagus, ALCHEMY Studies of Small Molecules, Selected Topics in Molecular Physics, Verlag Chemie (1972).

42. Program MOLECULE-CI by B. Roos and P. Siegbahn, University of Stockholm, Stockholm, Sweden.

43. H. F. Schaefer, The Electronic Structure of Atoms and Molecules: A Survey of Regorous Quantum Mechanical Results (Addison-Wesley, Reading, Mass., 1972).